Refraction-based tomosynthesis: Proof of the concept

Anton Maksimenko[a)]
High Energy Accelerator Research Organization (KEK), Oho 1-1, Tsukuba, Ibaraki, 305-0801, Japan and Faculty of Engineering, Yamagata University Yonezava, Yamagata 992, Japan

Tetsuya Yuasa
DDS Center, Tokyo University of Science, Yamasaki, Noda, Chiba 278-8510, Japan

Masami Ando
Faculty of Engineering, Yamagata University Yonezava, Yamagata 992-8510, Japan

Eiko Hashimoto
Ibaraki Prefectural University of Health Sciences, Ibaraki, 300-8510, Japan

(Received 19 September 2007; accepted 9 November 2007; published online 7 December 2007)

Tomosynthesis is a well known technique for imaging a plane in a target by blurring other planes in the target. Commonly, the tomosynthesis is based on the x-ray absorption contrast. Recently, methods for generating other x-ray contrasts were developed. One of them, the so-called refraction contrast, is extremely sensitive to soft tissues and small defects. It was used as the base for the computed tomography. However, a very promising application of this contrast in the tomosynthesis remains undeveloped. This letter is dedicated to this problem. It includes both theoretical background and experimental implementation of the idea. © *2007 American Institute of Physics*. [DOI: 10.1063/1.2819605]

Tomosynthesis (TS) is a three-dimensional (3D) digital technique that removes the effect of superimposed tissue.[1] Although the fundamental idea of TS was proposed in the 1930s, it had been hampered for decades because no suitable two-dimensional detectors existed. Nowadays, the TS is attracting more and more attention due to the recent development of the flat panel detector.[2] This method involves the acquisition of multiple images of an object from different angles during a short scan. TS is similar to the computed tomography (CT),[3] but unlike CT scans, which commonly use 180° revolutions, TS uses a smaller, selected number of angles producing section images which have superb spatial resolution in the plane of the image, but less resolution in the depth direction. The number of projections in the TS scan can be down to a few tens, which is one to two orders of magnitude smaller than that of the CT. Although the quality of the TS images is inferior to the CT, the tomographic information is obtained with much smaller radiation dose. The conventional TS is based on the absorption contrast. Interaction of the x-rays with a medium is determined by the complex refractive index $n=1-\delta+i\beta$, where β describes the absorption while the phase-shift term δ incorporates the refractive effects. The absorption-based x-ray imaging forms images by use of the imaginary part β. However, soft tissues which are of the main interest for the biomedical imaging mostly consist of elements with low atomic number. Coefficient β of these elements is usually so low in the hard x-ray region that the absorption-based imaging cannot produce enough contrast to differentiate various tissues, while the phase-shift term δ can be as much as 1000 times greater. Imaging techniques, which can visualize the phase-shift term, were rapidly developing in the last years (see Refs. 4–12 for example). They were followed by the applications in the CT.[13–17] Combining TS with the refraction-based imaging will produce a tomographic imaging method with an extremely low radiation dose and high sensitivity for soft tissues, which can be directly applied in the medical imaging.[18] This letter describes imaging principle and proof-of-concept experiment with the reference to the TS based on the refraction contrast. It includes both theoretical consideration of the problem and experimental realization. Refraction-based TS and CT reconstructions of two objects are presented as well as their absorption-based analogs for the comparison.

When an x-ray penetrates through an object it deflects on the boundaries of different tissue types and inner inhomogeneities. The deflection angle of the x-ray beam out of a certain plane (called the plane of the beam hereafter) as it penetrates through the subject is calculated as the integral over the beam path with the elemental deflection in the integrand[13–15]

$$\Delta\alpha = \int_S \frac{\partial\delta(\mathbf{r})}{\partial t} ds, \tag{1}$$

with $\mathbf{r}\equiv(x,y)$ being the coordinate of the point in the plane geometry, S is the integration path given by the straight line along the beam, and axis t is perpendicular to the plane of the beam. Typical deflection after the penetration is of the order of $10^{-5,\ldots,-7}$ radians for the hard x-ray since the value $\delta(\mathbf{r})$ is of the same order. In 1997, Chapman *et al.* presented diffraction enhanced imaging (DEI) method[10] which can visualize such small deflections and extract the "pure refraction" component from the mixture of the absorptions, small-angle scattering and refraction contrasts. Then the refraction contrast is used in the TS process.

One can note the similarity of Eq. (1) to the equation used for the absorption contrast (see Ref. 3 for example)

a)Electronic mail: antonmx@post.kek.jp.

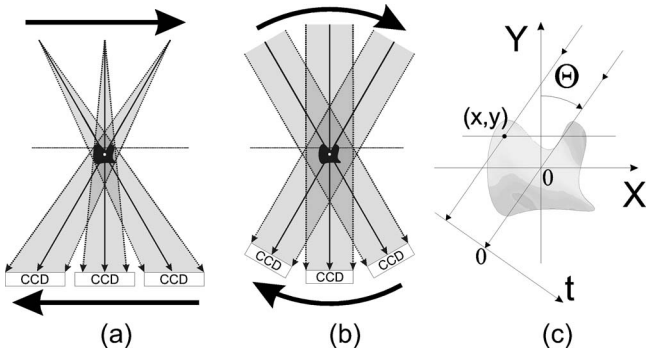

FIG. 1. Principal schemes of shift-and-add (a) and parallel beam (b) TS. (c) Parallel beam geometry.

$$ln\frac{I}{I_0} = \int_S \mu(\mathbf{r})ds. \tag{2}$$

Here, I and I_0 are the intensities of the x-ray beam before and after the object, respectively. $\mu(\mathbf{r})$ is the attenuation coefficient of the media. The difference between the equations for the refraction [Eq. (1)] and absorption [Eq. (2)] is the integrand function and the left part of the equality while the meaning is the same: "something experimentally measurable is equal to the ray integral of something else to be reconstructed." This allows adoption of the previously developed TS methods for the refraction contrast. We started with the easiest shift-and-add method[2] modifying it with respect to the geometry of the synchrotron beam and that of the refraction contrast. First of these modifications comes from the fact that the original shift-and-add algorithm was developed for the x-ray point-source geometry depicted in Fig. 1(a), while the refraction contrast requires the highly parallel x-ray beam [see Fig. 1(b)], which is currently available only from the synchrotron sources. This limits the choice of possible TS geometries to the case of the complete isocentric angle variation. As it is depicted in Fig. 1(c), the projection of the (x,y) point inside the object to the t axis (which corresponds to the detector) is given by $t=x\cos\Theta - y\sin\Theta$, where Θ is the rotation angle of the object. A TS image of the focal plane with coordinate y [dotted line in Fig. 1(c)] is the average of all projection images,

$$I_y(t) = \frac{1}{M}\sum_{m=1}^{M} I(x\cos\Theta_m - y\sin\Theta_m). \tag{3}$$

Here, M is the total number of projections and Θ_m is the rotation angle of the mth projection. In the above equation, member $y\sin\Theta_m$ represents the shift which must be imposed on the image. The first member $x\cos\Theta_m$ shows that the image must be shrinked before adding it. Therefore, the parallel geometry leads to the "shrink-shift-and-add" method instead of the "shift-and-add" used in the point-source geometry. The second peculiarity of our method comes from the nature of the refraction contrast. Equation (1) shows that the reconstructed function represents the gradient $\partial\delta(\mathbf{r})/\partial t$, while most users would prefer the results representing the real physical value $\delta(\mathbf{r})$. In order to convert the gradient to the field, we need to perform the integration of the $I_y(t)$ over the horizontal line. In practice, the integration takes the form of the summation over the pixels in each line.

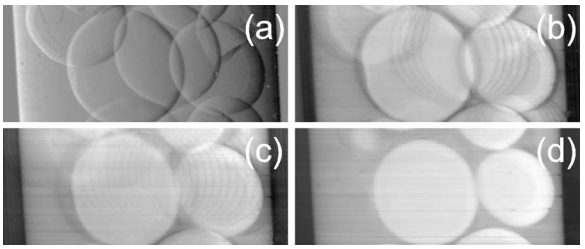

FIG. 2. (a) One example of the pure refraction contrast: the intensity is proportional to the deflection angle with the middle-gray corresponding to the zero deflection. TS reconstruction from (b) 5 and (c) 11 projections. (d) CT reconstruction from 1800 projections.

We performed the experiment to illustrate the theoretical approach described above. We used the vertical wiggler beamline BL14B at the Photon Factory, KEK, Japan. The experimental setup was designed in accordance with the DEI method.[10] Both crystals used Si(220) diffraction type and monochromator had asymmetry angle 9.5°, while the analyzer was symmetrically cut. The photon energy was set to 17.5 keV. The images taken on each side of the rocking curve were processed using the nonlinear extension of the original DEI (Ref. 2) (this extension considers the rocking curve of the analyzer as is intead of its linear approximation used in the original DEI). For these pilot experiments, we used a testing sample consisting of the nylon balls stored in oil. The size of the balls was 1.0 mm and the holder, a plastic pipe, had a 5 mm in diameter. One example of the pure refraction contrast is depicted in Fig. 2(a). The series of similar images taken at different rotations compose the set of TS projections. In all our experiments, we used 4° rotation step, which is the usual number for the mammography TS.[1,18] The first reconstruction was performed from five projections varying Θ within 16° arc. Reconstruction of one focal plane

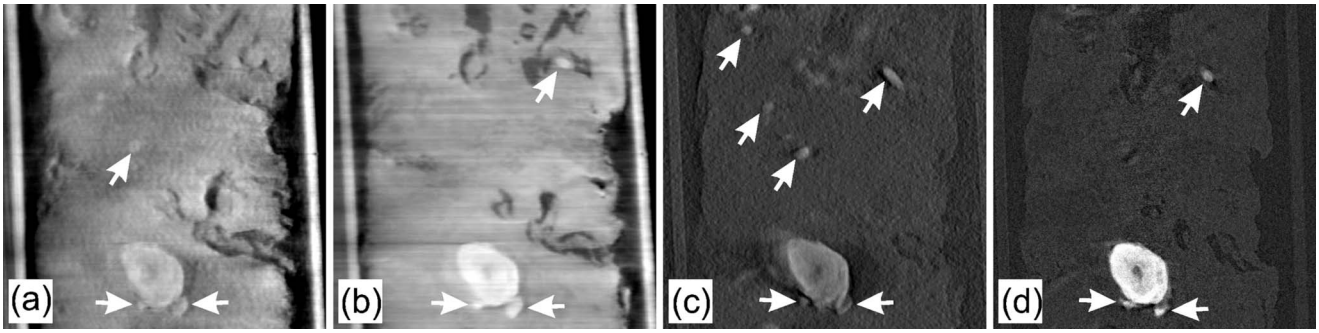

FIG. 3. Reconstruction of one plane of the breast cancer sample using (a) refraction TS, (b) refraction CT, (c) absorption TS, and (d) absorption CT. The color levels in the absorption images [(c) and (d)] were adjusted to enhance the contrast. Otherwise the contrast modulation would not exceed 7%. The white arrows on the figures denotes the visible calcifications.

inside the object is presented in Fig. 2(b). Comparing it to the initial refraction image we can note that the objects outside the focal plane are blurred and less intense while still visible as the shadows. Also, the gradient-to-field transformation made the contrast more realistic comparing to the moonlike refraction image in Fig. 2(a). In the second reconstruction, we used 11 projections with rotation arc 40°. The reconstruction of the same focal plane is depicted in Fig. 2(c). In this image, the out-of-plane objects manifest themselves only as the fringes, while the shadows found in previous reconstruction disappeared. Increasing the number of projections and the rotation arc may improve both spatial resolution and contrast modulation. We have also performed the refraction-based CT (see Ref. 16 for more details) of the same sample under the same experimental conditions. The number of CT projections was 1800. The CT reconstruction of the same focal plane can be found in Fig. 2(d). Of course, it looks more preferable comparing to the TS images because the fringes disappeared completely, the edges of the in-plane objects are very sharp, and the contrast modulation is higher. However, it is necessary to remember that the CT reconstruction requires at least one order larger data set, which makes the acquisition time and the radiation dose proportionally larger.

Another sample tested in the experiment was the real breast tissue containing cancer parts. The sample had semicylindrical shape of approximately 3 mm in diameter. The images of this sample were taken under the same experimental conditions. This sample has more complex structure and therefore we used 21 projections for the TS process. The acquisition arc was 80°. The result of the TS reconstruction is depicted in Fig. 3(a) together with the reference image obtained via the refraction-based CT in Fig. 3(b). The images show that the TS reconstruction could reveal almost all of the details available in the CT image. Although some parts are blurred and unclear in the TS image, the overall representation of the sample is realistic and reliable. Of course, the CT image is superior to the TS but the latter one is well enough to judge about the object's inner structure. Images in Fig. 3(c) and 3(d) represent the conventional absorption TS and CT reconstruction of the same sample. The absorption-based data acquisition was performed at the same experimental system but the analyzing crystal was removed and the change-coupled device camera was placed in the beam right after the object. One can note that the resulting images dramatically differ from the one obtained using the refraction contrast. Although calcium parts (denoted by arrows on the figures) as well as the cancer cell (large white spot at the bottom) are well observed in both types of contrast, other details of the inner structure are much less informative in the absorption images.

Concluding the above material, we can state that we have implemented the refraction-based TS. The realistic reconstruction of the object proved the expectations and encourages further development. The method looks very promising to material science and medicine due to the high sensitivity to the soft tissue contrast and the extremely low radiation dose.

This research is financially supported by a Grant-in-Aid for JSPS Research, a Grant-in-Aid for Exploratory research (No. 15654042), and a Grant-in-Aid for Scientific Research (A) (No. 18206011) from the Japanese Ministry of Education, Culture, Sports, Science, and Technology (MEXT)

[1] B. G. Ziedses des Plantes, Acta Radiol. **13**, 182 (1932).
[2] J. T. Dobbins III and D. J. Godfrey, Phys. Med. Biol. **48**, R65 (2003).
[3] A. C. Kak and M. Slaney, *Principles of Computerized Tomographic Imaging* (IEEE Press, New York, 1988), p. 50.
[4] U. Bonse and M. Hart, Appl. Phys. Lett. **6**, 155 (1965).
[5] T. J. Davis, D. Gao, T. E. Gureyev, A. W. Stevenson, and S. W. Wilkins, Nature (London) **373**, 595 (1995).
[6] A. Momose, T. Takeda, Y. Itai, and K. Hirano, Nat. Med. **2**, 473 (1996).
[7] V. N. Ingal and E. A. Beliaevskaya, J. Phys. D **28**, 2314 (1995).
[8] P. Cloetens, W. Ludwig, J. Baruchel, D. V. Dyck, J. V. Landuyt, J. P. Guigay, and M. Schlenker, Appl. Phys. Lett. **75**, 2912 (1999).
[9] A. Bravin, J. Phys. D **36**, A24 (2003).
[10] D. Chapman, W. Thomlinson, R. E. Johnston, D. Washburn, E. Pisano, N. Gmür, Z. Zhong, R. Menk, F. Arfelli, and D. Sayers, Phys. Med. Biol. **42**, 2015 (1997).
[11] M. Ando, K. Hyodo, H. Sugiyama, A. Maksimenko, W. Pattanasiriwisawa, K. Mori, J. Roberson, E. Rubenstein, Y. Tanaka, J. Chen, D. Xian, and Z. Xiaowei, Jpn. J. Appl. Phys. **41**, 4742 (2002).
[12] A. Maksimenko, Appl. Phys. Lett. **90**, 154106 (2007).
[13] F. A. Dilmanian, Z. Zhong, B. Ren, X. Y. Wu, L. D. Chapman, I. Orion, and W. C. Thomlinson, Phys. Med. Biol. **45**, 933 (2000).
[14] K. M. Pavlov, C. M. Kewish, J. R. Davis, and M. J. Morgan, J. Phys. D **34**, A168 (2001).
[15] M. Wernick, J. Brankov, D. Chapman, Y. Yang, C. Muehleman, Z. Zhong, and M. A. Anastasio, Proc. SPIE **5535**, 369 (2004).
[16] A. Maksimenko, M. Ando, H. Sugiyama, and T. Yuasa, Appl. Phys. Lett. **86**, 124105 (2005).
[17] J. G. Brankov, M. N. Wernick, Y. Yang, J. Li, C. Muehleman, Z. Zhong, and M. A. Anastasio, Med. Phys. **33**, 278 (2006).
[18] L. T. Niklason, B. T. Christian, L. E. Niklason, D. B. Kopans, D. E. Castleberry, B. H. Opsahl-Ong, C. E. Landberg, P. J. Slanetz, A. A. Giardino, R. Moore, D. Albagli, M. C. DeJule, P. F. Fitzgerald, D. F. Fobare, B. W. Giambattista, R. F. Kwasnick, J. Liu, S. J. Lubowski, G. E. Possin, J. F. Richotte, C. Y. Wei, and R. F. Wirth, Radiology **205**, 399 (1997).